

Meissner screening masses in gluonic phase

Michio Hashimoto* and Junji Jia†

Department of Applied Mathematics, University of Western Ontario, London, Ontario N6A 5B7, Canada

(Dated: February 9, 2022)

A numerical analysis for the Meissner mass in the simplest gluonic phase (the minimal cylindrical gluonic phase II) is performed in the framework of the gauged Nambu-Jona-Lasinio model with cold two-flavor quark matter. We derive Meissner mass formulae without using the numerical second derivative. It is revealed that the gapless mode yields a characterized contribution to the Meissner mass. We also find that there are large and positive contributions from the tree gluon potential term to the transverse modes of gluons. It is shown that the simplest gluonic phase resolves the chromomagnetic instability in a rather wide region.

PACS numbers: 12.38.-t, 11.15.Ex, 11.30.Qc

I. INTRODUCTION

Quark matter at sufficiently high density and low temperature is expected to be in a color superconducting state driven by the BCS mechanism [1, 2, 3]. This is analogous to the electron Cooper pairing in a superconducting metal. However, quarks, unlike electrons, have color and flavor degrees of freedom as well as spin, so that the phase structure is quite rich. In nature, deconfined quark matter might exist in the interior of neutron stars [4]. Thus the dynamics of the color superconductivity has been intensively studied [5].

Bulk matter in compact stars should be in equilibrium under the weak interaction (β -equilibrium), and be electrically and color neutral. The electric and color neutrality conditions play a crucial role in the dynamics of the quark pairing [6, 7, 8, 9]. In addition, the strange quark mass cannot be neglected in moderately dense quark matter as in the compact stars. Then a mismatch $\delta\mu$ between the Fermi momenta of the pairing quarks is induced.

As the mismatch $\delta\mu$ increases, the conventional color superconducting state tends to be destroyed. Before the complete destruction, however, the Meissner mass of gluons turns to be imaginary in the gapped (2SC) and gapless (g2SC) two-flavor color superconducting phases [10]: In the g2SC phase with the diquark gap $\Delta < \delta\mu$ the 8th gluon has an imaginary Meissner mass, while the Meissner masses for the 4-7th gluons are imaginary also in the 2SC phase $\delta\mu < \Delta < \sqrt{2}\delta\mu$. This chromomagnetic instability implies that there should exist a more stable vacuum other than the 2SC/g2SC phase. Later a chromomagnetic instability was found

also in the three-flavor gapless color-flavor locked (gCFL) phase [11, 12, 13]. One of the central issues in this field is to establish the genuine ground state for realistic values of $\delta\mu$. Besides the gluonic phase [14, 15], a number of other candidates for the true vacuum have been proposed [16, 17, 18, 19, 20, 21, 22, 23, 24, 25, 26].

Connected with the chromomagnetic instability, it was revealed that there appear tachyonic plasmons in the 4-7th and 8th gluonic channels [27]. It clearly shows that the physical vectorial excitations carry the instabilities and thus supports the scenario with gluon condensates (gluonic phase).

It is also known that the physical diquark excitation (the diquark Higgs mode) suffers from the Sarma instability [28] in the g2SC region, which corresponds to the negative mass squared of the diquark Higgs at zero momentum. Furthermore, it was found that the diquark Higgs mode has a negative velocity squared $v^2 < 0$ in the g2SC region [29]. A similar instability is also discussed in Refs. [30, 31]. This problem should be also resolved in the genuine ground state.

In Refs. [14, 15], the Ginzburg-Landau (GL) approach in the hard dense loop (HDL) approximation was employed in the vicinity of $\delta\mu \approx \Delta/\sqrt{2}$. Outside the scaling region around $\delta\mu \approx \Delta/\sqrt{2}$, the self-consistent analysis by solving the gap equations and the neutrality conditions was recently performed in Ref. [32]: It is shown that the gluonic phase is actually realized in a wide region of the parameter space and it is energetically more favorable than the normal, 2SC/g2SC, and the single plane wave Larkin-Ovchinnikov-Fulde-Ferrell (LOFF) [16, 33, 34] phases. It is also found that the values of Δ and $\delta\mu$ in the gluonic phase are significantly different from those in the 2SC/g2SC phase. It is noticeable that the values of the gluon condensate are large, say, $\mathcal{O}(100\text{--}250\text{MeV})$ in the almost whole region where it exists. On the other hand, the values of the color chemical potentials are relatively small. For the earlier works in

*Electronic address: mhashimo@uwo.ca

†Electronic address: jjia5@uwo.ca

other approaches, see Refs. [35, 36]. The extension to the model with nonzero temperature is studied in Ref. [37].

In this paper, we examine whether or not the gluonic phase resolves the chromomagnetic instability. We derive formulae for the Meissner mass without using the numerical second derivative. It turns out that the gapless mode gives a special contribution to the Meissner mass. In the numerical analysis, we consider the gluonic phase with the simplest ansatz which is called the minimal cylindrical gluonic phase II [15, 32]. As a benchmark, we also analyze the single plane wave LOFF and 2SC/g2SC phases including the non-HDL corrections.

We find that in the gluonic phase the tree gluon potential term yields positive and large contributions to the Meissner masses of the transverse modes of gluons. Actually, in the minimal cylindrical gluonic phase II, the chromomagnetic instability is resolved in the weak and intermediate coupling region, $65.4\text{MeV} < \Delta_0 < 130\text{MeV}$ for $\mu = 400\text{MeV}$ and $\Lambda = 653.3\text{MeV}$, where μ and Λ denote the quark chemical potential and the cutoff in the (gauged) Nambu-Jona-Lasinio (NJL) model, respectively. We here introduced the 2SC gap parameter Δ_0 defined at $\delta\mu = 0$, which essentially corresponds to the four-diquark coupling constant in the (gauged) NJL model. In the intermediate and strong coupling region $130\text{MeV} < \Delta_0 < 160\text{MeV}$, however, the chromomagnetic instability occurs in the transverse modes of the 4th and 5th gluons. Besides, in a small region around $\Delta_0 \simeq 150\text{MeV}$, the squared Meissner mass for the transverse mode of the 8th gluon becomes negative. For the other modes, the chromomagnetic instability does not occur. On the other hand, the single plane wave LOFF phase resolves the chromomagnetic instability only in the region $64.9\text{MeV} < \Delta_0 < 80\text{MeV}$. This is consistent with the results within the HDL approximation shown in Ref. [34]. Numerically, the 2SC phase suffers from the illness in $134.6\text{MeV} < \Delta_0 < 160\text{MeV}$, whereas the g2SC phase does in $\Delta_0 < 134.6\text{MeV}$. We thus conclude that the situation is definitely improved even in the simplest gluonic phase. If we consider more complicated gluonic phases such as the cylindrical gluonic phase I [14, 15] and/or the gluonic color-spin locked (GCSL) phase [15, 32], the chromomagnetic instability might be completely removed.

The paper is organized as follows: In Sec.II, the gauged NJL model is described. We also show the dynamical solutions of the gluonic, LOFF and 2SC/g2SC phases. In Sec.III A, we develop the formulae for the numerical calculation of the Meissner masses. We numerically analyze the Meissner masses for the gluonic, LOFF and 2SC/g2SC phases in Sec.III B. Section IV presents the summary and discussions.

II. MODEL

We study the gauged Nambu-Jona-Lasinio (NJL) model with two light quarks. We neglect the current quark masses and the $(\bar{\psi}\psi)^2$ -interaction channel. The Lagrangian density is given by

$$\mathcal{L} = \bar{\psi}(i\not{D} + \mu_0\gamma^0)\psi + G_\Delta \left[(\bar{\psi}^C i\varepsilon^\alpha \gamma_5 \psi)(\bar{\psi} i\varepsilon^\alpha \gamma_5 \psi^C) \right] - \frac{1}{4} F_{\mu\nu}^a F^{a\mu\nu}, \quad (1)$$

with

$$D_\mu \equiv \partial_\mu - igA_\mu^a T^a, \quad F_{\mu\nu}^a \equiv \partial_\mu A_\nu^a - \partial_\nu A_\mu^a + gf^{abc}A_\mu^b A_\nu^c, \quad (2)$$

where ε and ϵ^α are the totally antisymmetric tensors in the flavor and color spaces, respectively. We also introduced gluon fields A_μ^a , the QCD coupling constant g , the generators T^a of $SU(3)$, and the structure constants f^{abc} . The quark field ψ is a flavor doublet and color triplet. The charge-conjugate spinor is defined by $\psi^C \equiv C\bar{\psi}^T$ with $C = i\gamma^2\gamma^0$. We do not introduce the photon field. On the other hand, the whole theory contains free electrons, although we do not show them explicitly in Eq. (1). In β -equilibrium, the chemical potential matrix μ_0 for up and down quarks is

$$\mu_0 = \mu \mathbf{1} - \mu_e Q_{\text{em}}, \quad (3)$$

with $\mathbf{1} \equiv \mathbf{1}_c \otimes \mathbf{1}_f$, and $Q_{\text{em}} \equiv \mathbf{1}_c \otimes \text{diag}(2/3, -1/3)_f$, where μ and μ_e are the quark and electron chemical potentials, respectively. (The baryon chemical potential μ_B is given by $\mu_B \equiv 3\mu$.) The subscripts c and f mean that the corresponding matrices act on the color and flavor spaces, respectively. Hereafter, we abbreviate the unit matrices, $\mathbf{1}$, $\mathbf{1}_c$ and $\mathbf{1}_f$, if it is self-evident. By introducing the diquark field $\Phi^\alpha \sim i\bar{\psi}^C \varepsilon^\alpha \gamma_5 \psi$, we can rewrite the Lagrangian density (1) as

$$\mathcal{L} = \bar{\psi}(i\not{D} + \mu_0\gamma^0)\psi - \frac{|\Phi^\alpha|^2}{4G_\Delta} - \frac{1}{2}\Phi^\alpha [i\bar{\psi}\varepsilon^\alpha \gamma_5 \psi^C] - \frac{1}{2}[i\bar{\psi}^C \varepsilon^\alpha \gamma_5 \psi]\Phi^{*\alpha} - \frac{1}{4} F_{\mu\nu}^a F^{a\mu\nu}. \quad (4)$$

In the 2SC/g2SC phase, we can choose the anti-blue direction without loss of generality,

$$\langle \Phi^r \rangle = 0, \quad \langle \Phi^g \rangle = 0, \quad \langle \Phi^b \rangle = \Delta, \quad (5)$$

where the diquark condensate Δ is real. In this basis, by imposing the color neutrality condition, the color chemical potential μ_8 is induced [38]. We can interpret μ_8 as the vacuum expectation value (VEV) of the time component of the 8th gluon.

Let us define the Nambu-Gor'kov spinor,

$$\Psi \equiv \begin{pmatrix} \psi \\ \psi^C \end{pmatrix}. \quad (6)$$

The propagator inverse of Ψ in the 2SC/g2SC phase is given by

$$S^{-1}(P) = \begin{pmatrix} [G_0^+]^{-1} & \Delta^- \\ \Delta^+ & [G_0^-]^{-1} \end{pmatrix}, \quad (7)$$

with

$$[G_0^+]^{-1}(P) \equiv (p_0 + \bar{\mu} - \delta\mu\tau_3 - \mu_8\mathbf{1}_b)\gamma^0 - \vec{\gamma} \cdot \vec{p}, \quad (8)$$

$$[G_0^-]^{-1}(P) \equiv (p_0 - \bar{\mu} + \delta\mu\tau_3 + \mu_8\mathbf{1}_b)\gamma^0 - \vec{\gamma} \cdot \vec{p}, \quad (9)$$

and

$$\Delta^- \equiv -i\varepsilon\epsilon^b\gamma_5\Delta, \quad \Delta^+ \equiv \gamma^0(\Delta^-)^\dagger\gamma^0 = -i\varepsilon\epsilon^b\gamma_5\Delta, \quad (10)$$

where $P^\mu \equiv (p_0, \vec{p})$ is the energy-momentum four vector. We also defined $\tau_3 \equiv \text{diag}(1, -1)_f$, $\mathbf{1}_b \equiv \text{diag}(0, 0, 1)_c$, and

$$\bar{\mu} \equiv \mu - \frac{\delta\mu}{3} + \frac{\mu_8}{3}, \quad \delta\mu \equiv \frac{\mu_e}{2}. \quad (11)$$

The 2SC/g2SC phase is not the genuine ground state in the region $\delta\mu > \Delta/\sqrt{2}$, because it suffers from the chromomagnetic instability. A candidate to resolve the chromomagnetic instability is the gluonic phase with gluon condensates [14].

Let us introduce the gluon condensates $\langle A_\mu^a \rangle \neq 0$. When the space-component gluon condensates $\langle \vec{A}^a \rangle \neq 0$ are incorporated into the theory, the time-component VEVs of the gluon fields other than the 8th one are generally induced as well. We may interpret them as the color chemical potentials¹ [39]:

$$\mu_{\check{a}} = g\langle A_0^{\check{a}} \rangle, \quad (\check{a} = 1, 2, \dots, 7), \quad \mu_8 = \frac{\sqrt{3}}{2}g\langle A_0^8 \rangle. \quad (12)$$

The propagator inverse S_g^{-1} of Ψ including the gluon condensates is written as

$$S_g^{-1}(P) = \begin{pmatrix} [G_{0,g}^+]^{-1} & \Delta^- \\ \Delta^+ & [G_{0,g}^-]^{-1} \end{pmatrix}, \quad (13)$$

with

$$[G_{0,g}^+]^{-1}(P) \equiv (p_0 + \boldsymbol{\mu}_0)\gamma^0 - \vec{\gamma} \cdot \vec{p} + g\langle A^a \rangle T^a, \quad (14)$$

$$[G_{0,g}^-]^{-1}(P) \equiv (p_0 - \boldsymbol{\mu}_0)\gamma^0 - \vec{\gamma} \cdot \vec{p} - g\langle A^a \rangle (T^a)^T. \quad (15)$$

In the fermion one-loop approximation, the bare effective potential including both gluon and diquark condensates is given by

$$V_{\text{eff}}^{\text{bare}} = \frac{\Delta^2}{4G_\Delta} + \frac{1}{4}F_{\mu\nu}^a F^{a\mu\nu} - \frac{\mu_e^4}{12\pi^2} - \frac{1}{2} \int \frac{d^4P}{i(2\pi)^4} \text{Tr} \ln S_g^{-1}, \quad (16)$$

where we added the free electron contribution. Since the bare potential has a divergence, a counter term is required. We take into account only differences of the free energies with and without the chemical potentials. We thus define the renormalized effective potential by

$$V_{\text{eff}}^R \equiv V_{\text{eff}}^{\text{bare}} - V_{\text{c.t.}}, \quad (17)$$

with the counter term,

$$V_{\text{c.t.}} = -\frac{1}{2} \int \frac{d^4P}{i(2\pi)^4} \text{Tr} \ln S_g^{-1} \Big|_{\mu=\mu_e=\mu_a=0, \Delta=0, \langle \vec{A}^a \rangle \neq 0}. \quad (18)$$

In this prescription, even if we use the regularization scheme with the sharp cutoff Λ for the loop integral, we can remove artificial mass terms of gluons like $\Lambda^2 \vec{A}_a^2$.

In general, we can reduce the 32 homogeneous gluon condensates to 25 ones [15]. However the general case is quite complicated and hence it is difficult to find the self-consistent solutions of the gap equations and the color neutrality conditions for the 25 VEVs at present.

In this paper, we consider the minimal ansatz for the cylindrical gluonic phase II [15, 32],

$$\mu_3 \equiv g\langle A_0^3 \rangle, \quad \mu_8 \equiv \frac{\sqrt{3}}{2}g\langle A_0^8 \rangle, \quad B \equiv g\langle A_z^6 \rangle. \quad (19)$$

In order to make the physical meaning of the gluon condensates clearer, it is convenient to use the unitary gauge in which all gauge dependent degrees of freedom are removed. We shall fix the gauge as follows [15]:

$$\Phi^r \equiv 0, \quad \Phi^g \equiv 0, \quad \text{Im}\Phi^b \equiv 0, \quad (20)$$

and

$$A_z^4 \equiv 0, \quad A_z^5 \equiv 0, \quad A_z^7 \equiv 0. \quad (21)$$

As a benchmark, we also consider the single plane-wave 2SC-LOFF phase [16, 33, 34],

$$\langle \Phi^r \rangle = \langle \Phi^g \rangle = 0, \quad \langle \Phi^b \rangle = \Delta e^{-2i\vec{q} \cdot \vec{x}}. \quad (22)$$

¹ In an appropriate basis, the color chemical potentials can be reduced only into μ_3 and μ_8 , because the color chemical potential matrix $\boldsymbol{\mu}_c \equiv \mu_a T^a$ ($a = 1, 2, \dots, 8$) is hermite and traceless. In this case, however, the basis for the diquark field changes from Eq. (5).

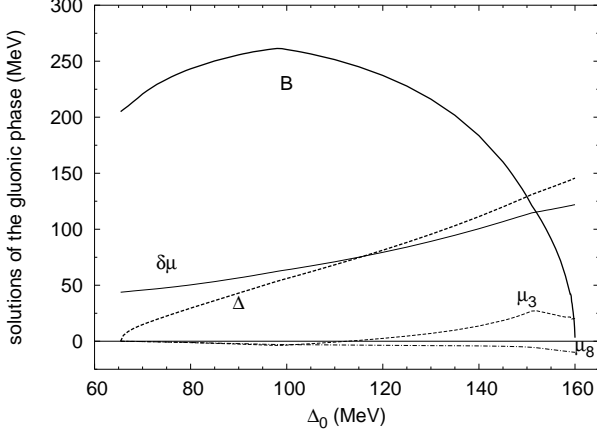


FIG. 1: The dynamical solutions for the minimal cylindrical gluonic phase II. The bold solid, bold dashed, thin solid, thin dashed and thin dot-dashed curves represent the values of B , Δ , $\delta\mu$, μ_3 and μ_8 , respectively. The values $\Lambda = 653.3$ MeV and $\mu = 400$ MeV were used. We also took $\alpha_s = 1$.

Introducing the quark field $\psi' = e^{i\vec{q}\cdot\vec{x}}\psi$ with the color-singlet phase, we can erase the x -dependent phase of the LOFF order parameter and instead, the x -independent color-singlet term $\bar{\psi}\vec{\gamma}\vec{q}\psi$ is induced in the kinetic term for quarks. Although the vector \vec{q} is also gauge equivalent to the condensate $\langle\vec{A}_8\rangle$, there is subtlety with respect to the tree gluon kinetic term: Notice that the tree gluon potential does not give any contribution to the free energy, while it is relevant to the Meissner masses for the transverse modes of the 4-7th gluons, because T^8 does not commute to T^{4-7} and thereby the corresponding Meissner masses are of the order of $q(\equiv |\vec{q}|)$. The point is that the values of q are large in a wide range of the parameter region where the LOFF phase exists, as we will see below. In order to avoid confusion, we may use the color-singlet transformation or *we simply do not incorporate the tree gluon potential term into the LOFF phase in any case.*

The dynamics of the minimal cylindrical gluonic phase II is analyzed in Ref. [32] by solving the gap equations and the neutrality conditions in a self-consistent way. We explicitly show the results for the gluonic, single plane wave LOFF and 2SC/g2SC phases in Figs.1–3, respectively. In the analysis, we took realistic values $\mu = 400$ MeV and $\Lambda = 653.3$ MeV. We also converted the four-diquark coupling constant G_Δ to the 2SC gap parameter Δ_0 defined at $\delta\mu = 0$ and varied the values of Δ_0 from the weak coupling regime ($\Delta_0 \sim 60$ MeV) to the strong coupling one ($\Delta_0 \sim 200$ MeV). For the gluonic phase, it is required to specify the value of $\alpha_s[\equiv g^2/(4\pi)]$, although the results for the minimal cylindrical gluonic phase II are not sensitive to the choice of the values of

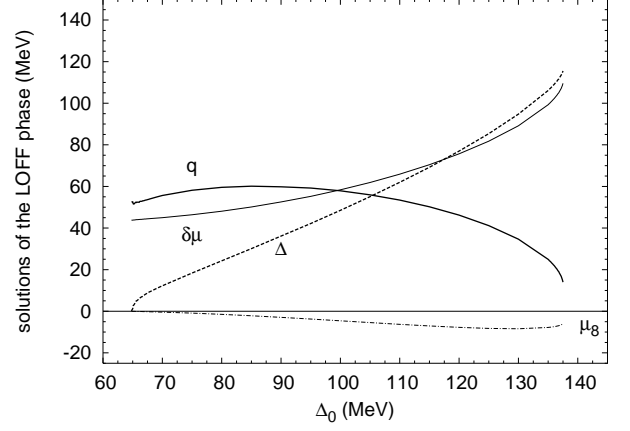


FIG. 2: The dynamical solutions for the single plane wave LOFF phase. The bold solid, bold dashed, thin solid and thin dot-dashed curves represent the values of q ($\equiv |\vec{q}|$), Δ , $\delta\mu$ and μ_8 , respectively. The values $\Lambda = 653.3$ MeV and $\mu = 400$ MeV were used.

α_s [32]. We here took $\alpha_s = 1$.

While the neutral normal phase without the diquark condensate always exists, the neutral gluonic, LOFF, g2SC and 2SC phases do only in the regions,

$$65.4\text{MeV} < \Delta_0 < 160\text{MeV}, \quad (\text{gluonic}) \quad (23)$$

$$64.9\text{MeV} < \Delta_0 < 138\text{MeV}, \quad (\text{LOFF}) \quad (24)$$

$$92.2\text{MeV} < \Delta_0 < 134.6\text{MeV}, \quad (\text{g2SC}) \quad (25)$$

and

$$\Delta_0 > 134.6\text{MeV}, \quad (\text{2SC}) \quad (26)$$

respectively.

The analysis for the free energies has been done in Ref. [32]: The normal phase is realized in the weak coupling regime with $\Delta_0 < 64.9$ MeV. While the single plane wave LOFF phase is energetically most favorable only in the narrow region $64.9\text{MeV} < \Delta_0 < 67\text{MeV}$, the minimal cylindrical gluonic phase II is stabler than the LOFF and 2SC/g2SC phases in the wide region $67\text{MeV} < \Delta_0 < 160\text{MeV}$. In the strong coupling regime with $\Delta_0 > 160\text{MeV}$, the 2SC phase is realized.

For the numerical calculation of the Meissner masses, we use the solutions shown in Figs.1–3. It is noticeable that the condensate B is large in the almost whole region where the gluonic phase exists. (See Fig. 1.) This feature is crucial for the Meissner masses in the gluonic phase, as we will see in the next section.

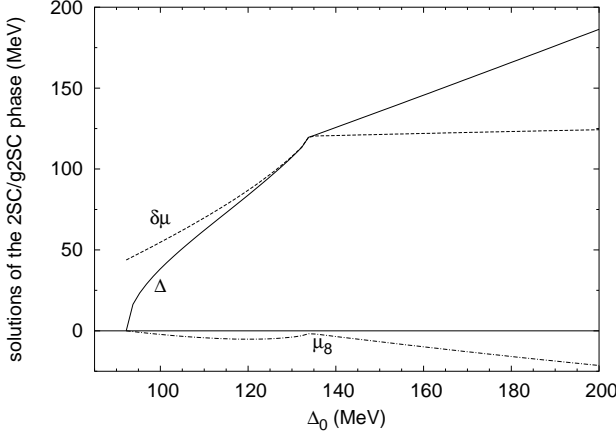


FIG. 3: The dynamical solutions for the 2SC/g2SC phase. The solid, dashed and dot-dashed curves represent the values of Δ , $\delta\mu$ and μ_8 , respectively. At $\Delta_0 = 134.6$ MeV, the g2SC phase turns into the 2SC one. The values $\Lambda = 653.3$ MeV and $\mu = 400$ MeV were used.

III. MEISSNER MASSES IN GLUONIC PHASE

A. Formulae

Let us derive formulae for the numerical calculation of the Meissner screening mass.

The squared Meissner mass can be expressed through the second derivative of the effective potential:

$$\frac{\partial^2 V_{\text{eff}}^R}{\partial A_\mu^a \partial A_\nu^b} = \Pi_{\text{tree}}^{\mu\nu} + \frac{g^2}{2} \int \frac{d^4 P}{i(2\pi)^4} \text{Tr} \left[S_g \Gamma^{\mu a} S_g \Gamma^{\nu b} \right] - \frac{g^2}{2} \int \frac{d^4 P}{i(2\pi)^4} \text{Tr} \left[S_g \Gamma^{\mu a} S_g \Gamma^{\nu b} \right]_{\text{c.t.}}, \quad (27)$$

where we defined the tree contribution

$$\begin{aligned} \Pi_{\text{tree}}^{\mu\nu} \equiv & g^2 f^{a_1 a b} f^{a_1 a_2 a_3} A^{a_2 \mu} A^{a_3 \nu} \\ & + g^2 f^{a_1 a a_2} f^{a_1 b a_3} g^{\mu\nu} A_\lambda^{a_2} A^{a_3 \lambda} \\ & + g^2 f^{a_1 a a_2} f^{a_1 a_3 b} A^{a_3 \mu} A^{a_2 \nu}, \end{aligned} \quad (28)$$

and the vertex

$$\Gamma^{\mu a} \equiv g^{-1} \frac{\partial S_g^{-1}}{\partial A_\mu^a} = \begin{pmatrix} \gamma^\mu T^a & 0 \\ 0 & -\gamma^\mu (T^a)^T \end{pmatrix}. \quad (29)$$

In Eq. (27), “c.t.” denotes the counter term and we used

$$0 = \frac{\partial}{\partial X} (S_g S_g^{-1}) = \frac{\partial S_g}{\partial X} S_g^{-1} + S_g \frac{\partial S_g^{-1}}{\partial X}, \quad (30)$$

for $X = A_\mu, \Delta, \delta\mu$, and linearity of S_g^{-1} with respect to all variables, i.e., $\frac{\partial^2 S_g^{-1}}{\partial X \partial Y} = 0$. We also abbreviated the bracket $\langle \dots \rangle$ for the gluon condensates.

For the numerical calculation, it is useful to diagonalize S_g^{-1} and/or S_g . Although the propagator inverse S_g^{-1} in Eq. (13) is a 48×48 matrix in the flavor, color, spinor and Nambu-Gor’kov spaces, we can block-diagonalize S_g^{-1} in the flavor and chirality spaces. This technique reduces our labour.

Let us transform the propagator inverse S_g^{-1} as follows;

$$S_g^{-1}(P) = \begin{pmatrix} \gamma^0 & 0 \\ 0 & i\varepsilon\gamma_5 \end{pmatrix} \tilde{S}_g^{-1}(P) \begin{pmatrix} 1 & 0 \\ 0 & -i\varepsilon\gamma^0\gamma_5 \end{pmatrix}, \quad (31)$$

with

$$\tilde{S}_g^{-1}(P) = p_0 \mathbf{1} + H_g, \quad H_g \equiv -\delta\mu\tau_3 + \begin{pmatrix} \bar{\mu} + \mu_c - \gamma^0 \vec{\gamma} \cdot \vec{p} - \gamma^0 \vec{\gamma} \cdot \vec{A} & \epsilon^b \Delta \\ -\epsilon^b \Delta & -\bar{\mu} - \mu_c^T + \gamma^0 \vec{\gamma} \cdot \vec{p} - \gamma^0 \vec{\gamma} \cdot \vec{A}^T \end{pmatrix}, \quad (32)$$

where

$$\bar{\mu} \equiv \mu - \frac{\delta\mu}{3}, \quad \mu_c \equiv gA_0^a T^a, \quad \vec{A} \equiv g\vec{A}^a T^a. \quad (33)$$

We here decomposed \tilde{S}_g^{-1} into the diagonal p_0 -part and the “Hamiltonian” H_g . (One can check easily hermiticity of H_g .) Notice that the flavor dependence of \tilde{S}_g^{-1} exists only in the first term of H_g and therefore \tilde{S}_g^{-1} is

flavor-diagonal. Since the inverse of Eq. (31) yields the expression for the propagator,

$$S_g(P) = \begin{pmatrix} 1 & 0 \\ 0 & i\varepsilon\gamma^0\gamma_5 \end{pmatrix} \tilde{S}_g(P) \begin{pmatrix} \gamma^0 & 0 \\ 0 & i\varepsilon\gamma_5 \end{pmatrix}, \quad (34)$$

the second derivative then reads

$$\frac{\partial^2 V_{\text{eff}}^R}{\partial A_\mu^a \partial A_\nu^b} = \Pi_{\text{tree}}^{\mu\nu} + \frac{g^2}{2} \int \frac{d^4 P}{i(2\pi)^4} \text{Tr} \left[\tilde{S}_g \tilde{\Gamma}^{\mu a} \tilde{S}_g \tilde{\Gamma}^{\nu b} \right] - \frac{g^2}{2} \int \frac{d^4 P}{i(2\pi)^4} \text{Tr} \left[\tilde{S}_g \tilde{\Gamma}^{\mu a} \tilde{S}_g \tilde{\Gamma}^{\nu b} \right]_{\text{c.t.}}, \quad (35)$$

with

$$\tilde{\Gamma}^{\mu a} \equiv \begin{pmatrix} \gamma^0 & 0 \\ 0 & i\varepsilon\gamma_5 \end{pmatrix} \Gamma^{\mu a} \begin{pmatrix} 1 & 0 \\ 0 & i\varepsilon\gamma^0\gamma_5 \end{pmatrix}, \quad (36)$$

$$= \begin{pmatrix} \gamma^0 \gamma^\mu T^a & 0 \\ 0 & -\gamma^\mu \gamma^0 (T^a)^T \end{pmatrix}. \quad (37)$$

Since the current quark masses are ignored, the theory is chiral invariant. Thus we can decompose the vertex and also the propagator into the right and left-handed parts.

One can easily show that the trace over the spinor space in Eq. (35) is the sum of the two parts.

In virtue of hermiticity, we can diagonalize H_g and \tilde{S}_g by a unitary matrix U ,

$$H_g = U H_{\text{diag}} U^\dagger, \quad H_{\text{diag}} = \text{diag}(E_1^\tau, E_2^\tau, \dots, E_n^\tau), \quad (38)$$

$$\tilde{S}_g = U \text{diag} \left(\frac{1}{p_0 + E_1^\tau}, \frac{1}{p_0 + E_2^\tau}, \dots, \frac{1}{p_0 + E_n^\tau} \right) U^\dagger, \quad (39)$$

where $\tau = \pm$ for $\tau_3 = \pm 1$ and $E_{1,2,\dots,n}^\tau$ denote the energy eigenvalues. It is not difficult to find *numerically* the energy eigenvalues and the unitary matrix by using a standard method. Noting that the integrand of Eq. (35) contains the p_0 -dependence only in \tilde{S}_g with the expression (39), we can explicitly perform the integral over p_0 and thereby obtain

$$\begin{aligned} \frac{\partial^2 V_{\text{eff}}^R}{\partial A_\mu^a \partial A_\nu^b} &= \Pi_{\text{tree}}^{\mu\nu} - \frac{g^2}{2} \sum_{\tau=\pm} \sum_{E_i^\tau \neq E_j^\tau} \int \frac{d^3 p}{(2\pi)^3} \frac{\theta(E_i^\tau) - \theta(E_j^\tau)}{E_i^\tau - E_j^\tau} (U^\dagger \tilde{\Gamma}^{\mu a} U)_{ij} (U^\dagger \tilde{\Gamma}^{\nu b} U)_{ji} \\ &\quad - \frac{g^2}{2} \sum_{\tau=\pm} \sum_{E_i^\tau = E_j^\tau} \int \frac{d^3 p}{(2\pi)^3} \delta(E_i^\tau) (U^\dagger \tilde{\Gamma}^{\mu a} U)_{ij} (U^\dagger \tilde{\Gamma}^{\nu b} U)_{ji} - (\text{counter term}). \end{aligned} \quad (40)$$

We can derive similar formulae for other second derivatives,

$$\frac{\partial^2 V_{\text{eff}}^R}{(\partial \Delta)^2}, \quad \frac{\partial^2 V_{\text{eff}}^R}{(\partial \mu_e)^2}, \quad \frac{\partial^2 V_{\text{eff}}^R}{\partial \Delta \partial A_\mu^a}, \quad \text{etc..} \quad (41)$$

It is also straightforward to extend the formulae to the version with a finite temperature.

The formula (40) has an advantage over the numerical derivative of the effective potential: The numerical second derivative requires a quite precise calculation for the free energy and thereby it takes a long time. On the other hand, we can reach a sufficiently accurate result via (40) in a reasonable time. Furthermore, in the expression of (40), it is clear that the contributions of the gapped and gapless modes to the Meissner masses are quite different. (Compare the second and third terms in Eq. (40).) This might help us to understand why the existence of the gapless modes yields a sudden change of the squared Meissner mass for the 8th gluon at the border of the 2SC and g2SC phases [10].

B. Numerical analysis

Before the numerical calculation, we describe several features of the Meissner masses in the minimal cylindrical gluonic phase II.

In this phase, the symmetry breaking structure is [15]

$$[SU(3)_c]_{\text{local}} \times U(1)_{\text{em}} \times SO(3)_{\text{rot}} \xrightarrow{\Delta, B} \tilde{U}(1)_{\text{em}} \times SO(2)_{\text{rot}}, \quad (42)$$

where the unbroken $\tilde{U}(1)_{\text{em}}$ is connected with the new electric charge $\tilde{Q}_{\text{em}} = Q_{\text{em}} - \frac{1}{\sqrt{3}} T^8 - T^3$. The rotational symmetry breaking leads to different Meissner masses for the transverse ($\mu, \nu = x, y$) and longitudinal ($\mu, \nu = z$) modes. It is thus convenient to define

$$(M^2)_{ab}^T \equiv \frac{\partial^2 V_{\text{eff}}^R}{\partial A_x^a \partial A_x^b} = \frac{\partial^2 V_{\text{eff}}^R}{\partial A_y^a \partial A_y^b}, \quad (43)$$

$$(M^2)_{ab}^L \equiv \frac{\partial^2 V_{\text{eff}}^R}{\partial A_z^a \partial A_z^b}. \quad (44)$$

Since we took the unitary gauge (21), the squared Meiss-

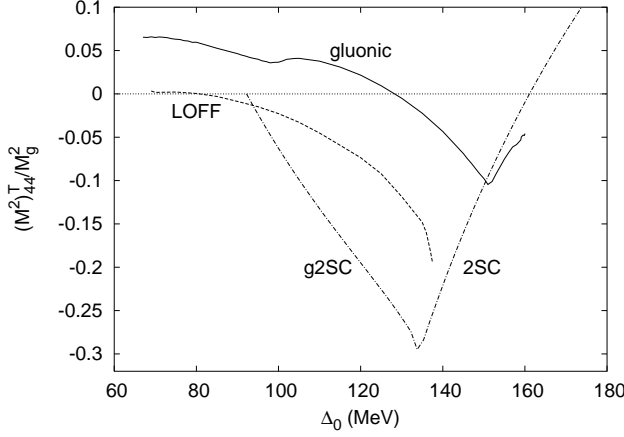


FIG. 4: The squared Meissner masses of the transverse mode of the 4th gluon in the unit of $M_g^2 [\equiv 4\alpha_s\mu^2/(3\pi)]$. The bold solid, dashed and dot-dashed curves are for the minimal cylindrical gluonic phase II, the single plane-wave LOFF and the 2SC/g2SC phases, respectively. The values $\Lambda = 653.3$ MeV, $\mu = 400$ MeV and $\alpha_s = 1$ were used.

ner masses for the physical degrees of freedom are

$$(M^2)^{T,L}_{11} = (M^2)^{T,L}_{22}, \quad (M^2)^T_{44} = (M^2)^T_{55}, \quad (45)$$

and

$$(M^2)^{T,L}_{33}, \quad (M^2)^{T,L}_{66}, \quad (M^2)^T_{77}, \quad (M^2)^{T,L}_{88}, \quad (46)$$

where the relations (45) hold owing to the unbroken $\tilde{U}(1)_{\text{em}}$ symmetry. For the transverse modes of the 3rd and 8th gluons, it turns out that there exists a large mixing term $(M^2)^T_{38}$, so that we define the diagonal mass-squared terms for them,

$$(M^2)^T_{33,\text{diag}}, \quad (M^2)^T_{88,\text{diag}}. \quad (47)$$

Do there exist two Nambu-Goldstone (NG) bosons connected with the symmetry breaking $SO(3)_{\text{rot}} \rightarrow SO(2)_{\text{rot}}$? This is nontrivial because Goldstone's theorem for relativistically invariant theories is not necessarily valid in noninvariant systems [40, 41]. We find that the answer is formally “yes” in this case, as we will see below.

The point is that the rotational symmetry is spontaneously broken only by the condensate $\langle A_z^6 \rangle \neq 0$ in the minimal cylindrical gluonic phase II. Therefore, before taking the z -direction, the effective potential should depend on the $SO(3)_{\text{rot}}$ invariant

$$B \equiv \sum_{i=x,y,z} \langle A_i^6 \rangle^2, \quad (48)$$

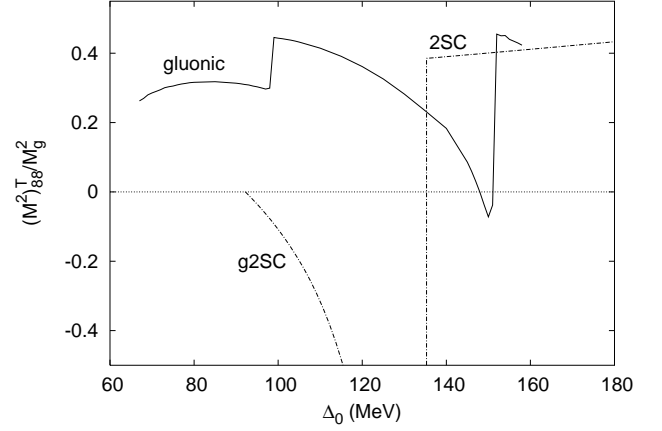


FIG. 5: The squared Meissner masses of the transverse mode of the 8th gluon in the unit of $M_g^2 [\equiv 4\alpha_s\mu^2/(3\pi)]$. The bold solid and dot-dashed curves are for the minimal cylindrical gluonic phase II and the 2SC/g2SC phases, respectively. The values $\Lambda = 653.3$ MeV, $\mu = 400$ MeV and $\alpha_s = 1$ were used. In the g2SC phase, the squared Meissner mass monotonously decreases and goes to minus infinity at $\Delta_0 = 134.6$ MeV, although it is not explicitly shown here.

i.e.,

$$V_{\text{eff}}^R = V_{\text{eff}}^R(B). \quad (49)$$

We then find

$$\frac{\partial^2 V_{\text{eff}}^R}{\partial \langle A_i^6 \rangle \partial \langle A_j^6 \rangle} = 2\delta_{ij} \frac{\partial V_{\text{eff}}^R}{\partial B} + 4\langle A_i^6 \rangle \langle A_j^6 \rangle \frac{\partial^2 V_{\text{eff}}^R}{(\partial B)^2}. \quad (50)$$

Since we take the direction $\langle A_{x,y}^6 \rangle = 0$, $\langle A_z^6 \rangle \neq 0$ and the gap equation for $\langle A_z^6 \rangle$ yields $\frac{\partial V_{\text{eff}}^R}{\partial B} = 0$, we formally find that the squared Meissner mass for the transverse mode of the 6th gluon is vanishing,

$$(M^2)^T_{66} = 0. \quad (51)$$

It implies that $A_{x,y}^6$ correspond to the two NG bosons.

A crucial difference between the gluonic and 2SC/g2SC phases is the existence of the tree gluon potential term. Although the effect is negligible for the free energy in the minimal cylindrical gluonic phase II, it is quite important for the Meissner masses. Neglecting the suppressed terms $\sim \mathcal{O}(\mu_3^2)$, $\mathcal{O}(\mu_3\mu_8)$, $\mathcal{O}(\mu_8^2)$, we obtain the tree terms of the squared Meissner masses:

$$(M^2)^T_{11,22} \simeq (M^2)^T_{44,55} \simeq (M^2)^T_{33} = \frac{B^2}{4}, \quad (52a)$$

$$(M^2)^T_{77} \simeq B^2, \quad (M^2)^T_{88} = \frac{3}{4}B^2, \quad (52b)$$

$$(M^2)^T_{38} = -\frac{\sqrt{3}}{4}B^2. \quad (52c)$$

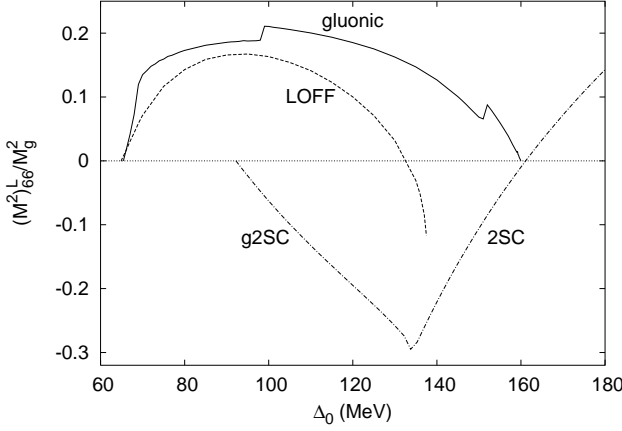


FIG. 6: The squared Meissner masses of the longitudinal mode of the 6th gluon in the unit of $M_g^2 \equiv 4\alpha_s\mu^2/(3\pi)$. The bold solid, dashed and dot-dashed curves are for the minimal cylindrical gluonic phase II, the single plane-wave LOFF and the 2SC/g2SC phases, respectively. The values $\Lambda = 653.3\text{MeV}$, $\mu = 400\text{MeV}$ and $\alpha_s = 1$ were used.

Thus the transverse modes except for $(M^2)_{66}^T$ and $(M^2)_{33,\text{diag}}^T$ have the *positive and large* contributions of the order of B^2 . (For the values of B , see Fig. 1.) This is one of the reasons why the Meissner masses tend to be positive compared with those in the 2SC/g2SC phase.

We also note some features of the Meissner masses for the single-plane wave 2SC-LOFF phase. The A_μ^{1-3} gluons should be massless and the relations

$$(M^2)_{44}^{T,L} = (M^2)_{55}^{T,L} = (M^2)_{66}^{T,L} = (M^2)_{77}^{T,L} \quad (53)$$

hold because of the unbroken $SU(2)_c$ gauge symmetry. In addition, similarly to (51), we formally obtain

$$(M^2)_{88}^T = 0. \quad (54)$$

Let us now turn to the numerical analysis of the Meissner masses.

We depict the results in Figs.4–8 in the unit of $M_g^2 \equiv 4\alpha_s\mu^2/(3\pi)$. In the analysis, we used $\mu = 400\text{MeV}$, $\Lambda = 653.3\text{MeV}$ and $\alpha_s = 1$.

For the minimal cylindrical gluonic phase II, the squared Meissner masses $(M^2)_{44}^T = (M^2)_{55}^T$ are positive in the region $65.4\text{MeV} < \Delta_0 < 130\text{MeV}$, while it suffers from the chromomagnetic instability in $130\text{MeV} < \Delta_0 < 160\text{MeV}$. (See Fig.4.) We also find that $(M^2)_{88}^T$ becomes negative in the small region around $\Delta_0 \sim 150\text{MeV}$. (See Fig.5.) For the other modes, however, the chromomagnetic instability does not occur as shown in Figs.6–8. (After the diagonalization of $(M^2)_{33}^T$, $(M^2)_{38}^T$ and $(M^2)_{88}^T$, the instability in $(M^2)_{88}^T$ is converted into $(M^2)_{33,\text{diag}}^T$,

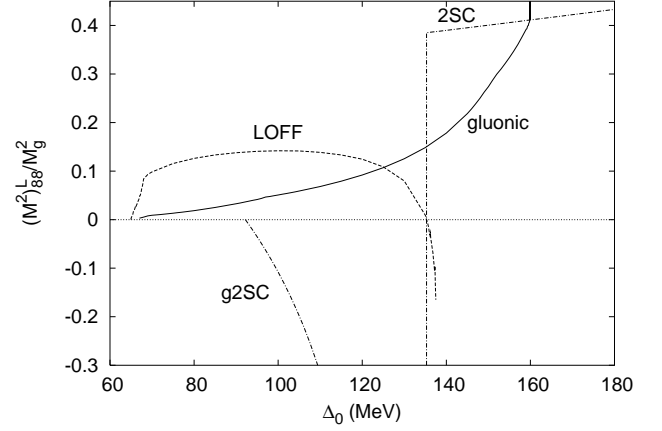


FIG. 7: The squared Meissner masses of the longitudinal mode of the 8th gluon in the unit of $M_g^2 \equiv 4\alpha_s\mu^2/(3\pi)$. The bold solid, dashed and dot-dashed curves are for the minimal cylindrical gluonic phase II, the single plane-wave LOFF and the 2SC/g2SC phases, respectively. The values $\Lambda = 653.3\text{MeV}$, $\mu = 400\text{MeV}$ and $\alpha_s = 1$ were used. As in Fig.5, the curve for the g2SC phase below the figure is cut off.

because we define the diagonalized squared masses as $(M^2)_{33,\text{diag}}^T < (M^2)_{88,\text{diag}}^T$.) It is quite noticeable that there exist spikes and valleys around $\Delta_0 \sim 100\text{MeV}$ and $\Delta_0 \sim 150\text{MeV}$ in Figs.4–6.

How about the sensitivity of the Meissner masses on α_s ? Although the dynamical solutions of Δ , B , $\delta\mu$, μ_3 and μ_8 in the minimal cylindrical gluonic phase II are almost independent of α_s [32], the Meissner masses for the transverse modes can be sensitive. Note that the one-loop contributions are proportional to α_s and thus the influence of the tree contributions (52) is relatively stronger (weaker) as the values of α_s decrease (increase). For example, $(M^2)_{44}^T$ becomes negative at $\Delta_0 = 140, 130, 120\text{MeV}$ for $\alpha_s = 0.85, 1.0, 1.15$, respectively. For the other transverse modes in Eq. (52), there should appear similar sensitivities. On the other hand, for the longitudinal modes, the ratio $(M^2)_{ab}^L/M_g^2$ is insensitive to α_s , because the tree contributions are suppressed.

For the single plane wave LOFF phase, like in the minimal cylindrical gluonic phase II, the transverse modes of the 4–7th gluons are the most problematic. However the chromomagnetic instability occurs in the earlier region, $80\text{MeV} < \Delta_0 < 138\text{MeV}$. (See Fig.4.) All the other modes also suffer from the chromomagnetic instability in the end of the LOFF phase around $\Delta_0 \sim 130\text{MeV}$. (See Fig.6 and 7.) This is different from the situation in the minimal cylindrical gluonic phase II. We also note that

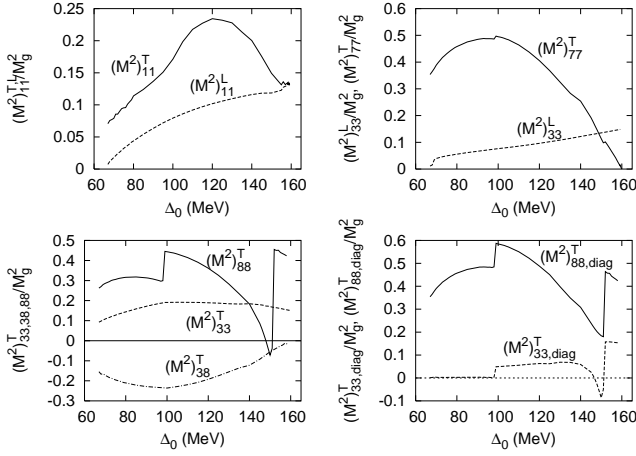


FIG. 8: The squared Meissner masses for several gluonic modes in the minimal cylindrical gluonic phase II in the unit of $M_g^2 \equiv 4\alpha_s \mu^2 / (3\pi)$. The values $\Lambda = 653.3\text{MeV}$, $\mu = 400\text{MeV}$ and $\alpha_s = 1$ were used. In the right bottom figure, we showed the diagonalized mass squared terms for the transverse modes of the 3rd and 8th gluons.

these results are consistent with the analysis based on the HDL approximation [33, 34].

The 2SC/g2SC phase has the chromomagnetic instability numerically in the region $92.2\text{MeV} < \Delta_0 < 160\text{MeV}$. The results agree with those in Appendix B in the second paper of Ref. [10] (, see also Refs. [42, 43]).

In conclusion, although the minimal cylindrical gluonic phase II does not completely remove the chromomagnetic instability, it cures the situation in a wide region.

The comments about the massless modes are in order. The numerical calculations including the non-HDL effects do not necessarily reproduce the vanishing Meissner masses. This fact is known even in the 2SC phase, i.e., the A_μ^{1-3} gluons acquire the non-HDL contributions like $\Delta^2 \log \Lambda^2 / \Delta^2$ in the sharp-cutoff regularization scheme [12, 44]. In order to settle this problem, a more sophisticated regularization scheme is required. It will be studied elsewhere.

IV. SUMMARY AND DISCUSSIONS

We analyzed the Meissner screening masses in the simplest gluonic phase (the minimal cylindrical gluonic phase II) as well as the single plane wave LOFF and 2SC/g2SC phases. We derived the formulae for the Meissner masses without any help of the numerical derivative. It was found that in the formulae the gapless mode makes the contribution characterized by the Dirac's δ -function. We showed that the simplest gluonic

phase removes the chromomagnetic instability in the region $65.4\text{MeV} < \Delta_0 < 130\text{MeV}$, whereas the single plane wave LOFF one does in $64.9\text{MeV} < \Delta_0 < 80\text{MeV}$. We here took $\Lambda = 653.3\text{MeV}$, $\mu = 400\text{MeV}$ and $\alpha_s = 1$. The 2SC phase does not have the chromomagnetic instability in the strong coupling regime $\Delta_0 > 160\text{MeV}$. Incorporating the analysis of the free energy [32], we conclude that in the region $67\text{MeV} < \Delta_0 < 130\text{MeV}$ the simplest ansatz for the gluonic phases works more nicely than the single plane wave LOFF and g2SC phases. On the other hand, the single plane wave LOFF phase is energetically more favorable and also resolves the chromomagnetic instability only in the window $64.9\text{MeV} < \Delta_0 < 67\text{MeV}$.

Furthermore, we found the noticeable behaviours of the squared Meissner masses in the minimal cylindrical gluonic phase II around $\Delta_0 \sim 100\text{MeV}$ and $\Delta_0 \sim 150\text{MeV}$. (See Figs.4–6.) The 2SC/g2SC phase also has the similar behaviours: Notice that there appears the abrupt change of the Meissner mass for the 8th gluon from the g2SC side to the 2SC one and that the values of the squared Meissner mass for the 4-7th gluons have the valley at the phase transition point from the g2SC phase to the 2SC one, as shown in Figs.4–7. These similarities might suggest that new gapless modes in the minimal cylindrical gluonic phase II appear around $\Delta_0 \sim 100\text{MeV}$ and $\Delta_0 \sim 150\text{MeV}$. We also note that the value of B takes its maximum around $\Delta_0 \sim 100\text{MeV}$ and that the relation $B \simeq \delta\mu$ is satisfied around $\Delta_0 \sim 150\text{MeV}$. (See Fig.1.) These facts might be significant. The dispersion relation for quarks in the gluonic phase will be performed elsewhere.

There still exists a chromomagnetically unstable region. However it should be noticed that we examined only the simplest ansätze for the LOFF and gluonic phases in this paper. The multiple plane wave LOFF phase may completely remove the chromomagnetic instability in the whole parameter region [17, 26]. More involved gluonic phases can also resolve the instability: Since there appears the illness in the transverse mode of the 4th gluon, the GCSL phase with the gluon condensates $\mu_8 = \sqrt{3}/2g\langle A_0^8 \rangle$ and $K = g\langle A_y^4 \rangle = g\langle A_z^6 \rangle$ [15, 32] is hopeful, for example. An important point is that the free energy for the GCSL phase is slightly lower than that for the minimal cylindrical gluonic phase II [32]. Inhomogeneous gluonic phases are also interesting [27, 45].

Independently of the chromomagnetic instability, the Sarma instability for the diquark Higgs mode should be removed as well. This problem will be considered elsewhere.

Acknowledgments

The authors thank V. A. Miransky for fruitful discussions. J.J. acknowledges useful discussions with Razvan

Nistor. The numerical calculations were carried out on Altix3700 BX2 at YITP in Kyoto University. The work was supported by the Natural Sciences and Engineering Research Council of Canada.

-
- [1] D. Bailin and A. Love, Phys. Rept. **107**, 325 (1984).
 - [2] M. Iwasaki and T. Iwado, Phys. Lett. B **350**, 163 (1995).
 - [3] M. G. Alford, K. Rajagopal and F. Wilczek, Phys. Lett. B **422**, 247 (1998); R. Rapp, T. Schäfer, E. V. Shuryak and M. Velkovsky, Phys. Rev. Lett. **81**, 53 (1998).
 - [4] D. Ivanenko and D. F. Kurdgelaidze, Astrofiz. **1**, 479 (1965); Lett. Nuovo Cim. **2**, 13 (1969); N. Itoh, Prog. Theor. Phys. **44**, 291 (1970); F. Iachello, W. D. Langer and A. Lande, Nucl. Phys. A **219**, 612 (1974).
 - [5] For a recent comprehensive review, see, e.g., M. G. Alford, K. Rajagopal, T. Schaefer and A. Schmitt, hep-ph/0709.4635.
 - [6] K. Iida and G. Baym, Phys. Rev. D **63**, 074018 (2001) [Erratum-ibid. D **66**, 059903 (2002)].
 - [7] M. Alford and K. Rajagopal, JHEP **0206**, 031 (2002).
 - [8] A. W. Steiner, S. Reddy and M. Prakash, Phys. Rev. D **66**, 094007 (2002).
 - [9] M. Huang, P. f. Zhuang and W. q. Chao, Phys. Rev. D **67**, 065015 (2003).
 - [10] M. Huang and I. A. Shovkovy, Phys. Rev. D **70**, 051501(R) (2004); *ibid* **70**, 094030 (2004).
 - [11] R. Casalbuoni, R. Gatto, M. Mannarelli, G. Nardulli and M. Ruggieri, Phys. Lett. B **605**, 362 (2005) [Erratum-ibid. B **615**, 297 (2005)].
 - [12] M. Alford and Q. Wang, J. Phys. G **31**, 719 (2005).
 - [13] K. Fukushima, Phys. Rev. D **72**, 074002 (2005).
 - [14] E. V. Gorbar, M. Hashimoto and V. A. Miransky, Phys. Lett. B **632**, 305 (2006).
 - [15] E. V. Gorbar, M. Hashimoto and V. A. Miransky, Phys. Rev. D **75**, 085012 (2007).
 - [16] M. G. Alford, J. A. Bowers and K. Rajagopal, Phys. Rev. D **63**, 074016 (2001). For a review, see, e.g., R. Casalbuoni and G. Nardulli, Rev. Mod. Phys. **76**, 263 (2004).
 - [17] J. A. Bowers and K. Rajagopal, Phys. Rev. D **66**, 065002 (2002).
 - [18] S. Reddy and G. Rupak, Phys. Rev. C **71**, 025201 (2005).
 - [19] M. Huang, Phys. Rev. D **73**, 045007 (2006).
 - [20] D. K. Hong, hep-ph/0506097.
 - [21] A. Kryjevski, hep-ph/0508180.
 - [22] T. Schäfer, Phys. Rev. Lett. **96**, 012305 (2006).
 - [23] R. Casalbuoni, R. Gatto, N. Ippolito, G. Nardulli and M. Ruggieri, Phys. Lett. B **627**, 89 (2005) [Erratum-ibid. B **634**, 565 (2006)].
 - [24] K. Rajagopal and R. Sharma, Phys. Rev. D **74**, 094019 (2006).
 - [25] M. Mannarelli, K. Rajagopal and R. Sharma, hep-ph/0702021.
 - [26] R. Gatto and M. Ruggieri, Phys. Rev. D **75**, 114004 (2007).
 - [27] E. V. Gorbar, M. Hashimoto, V. A. Miransky and I. A. Shovkovy, Phys. Rev. D **73**, 111502(R) (2006).
 - [28] G. Sarma, J. Phys. Chem. Solids **24**, 1029 (1963).
 - [29] M. Hashimoto, Phys. Lett. B **642**, 93 (2006).
 - [30] K. Iida and K. Fukushima, Phys. Rev. D **74**, 074020 (2006).
 - [31] I. Giannakis, D. Hou, M. Huang and H. c. Ren, Phys. Rev. D **75**, 011501(R) (2007); *ibid* **75**, 014015 (2007).
 - [32] M. Hashimoto and V. A. Miransky, Prog. Theor. Phys. **118**, 303 (2007).
 - [33] I. Giannakis and H. C. Ren, Phys. Lett. B **611**, 137 (2005); Nucl. Phys. B **723**, 255 (2005); I. Giannakis, D. f. Hou and H. C. Ren, Phys. Lett. B **631**, 16 (2005).
 - [34] E. V. Gorbar, M. Hashimoto and V. A. Miransky, Phys. Rev. Lett. **96**, 022005 (2006).
 - [35] K. Fukushima, Phys. Rev. D **73**, 094016 (2006).
 - [36] O. Kiriyama, D. H. Rischke and I. A. Shovkovy, Phys. Lett. B **643**, 331 (2006).
 - [37] O. Kiriyama, hep-ph/0709.1083.
 - [38] A. Gerhold and A. Rebhan, Phys. Rev. D **68**, 011502(R) (2003); D. D. Dietrich and D. H. Rischke, Prog. Part. Nucl. Phys. **53**, 305 (2004).
 - [39] M. Buballa and I. A. Shovkovy, Phys. Rev. D **72**, 097501 (2005).
 - [40] H. B. Nielsen and S. Chadha, Nucl. Phys. B **105**, 445 (1976).
 - [41] V. A. Miransky and I. A. Shovkovy, Phys. Rev. Lett. **88**, 111601 (2002); T. Schafer, D. T. Son, M. A. Stephanov, D. Toublan and J. J. M. Verbaarschot, Phys. Lett. B **522**, 67 (2001).
 - [42] O. Kiriyama, Phys. Rev. D **74**, 074019 (2006); *ibid* **74**, 114011 (2006).
 - [43] L. He, M. Jin and P. Zhuang, Phys. Rev. D **75**, 036003 (2007).
 - [44] D. H. Rischke, Phys. Rev. D **62**, 034007 (2000).
 - [45] E. J. Ferrer and V. de la Incera, hep-ph/0705.2403.